

Analysis of Steady-State MHD Free Convection of An Exothermic Fluid with Partial Slip and Suction/Injection

¹Hussaini A., ²Isah B. Y., ¹Zayyanu S. Y.

¹Sokoto State University, Sokoto

²Usmanu Danfodiyo University, Sokoto

Abstract— Analytical solution for entropy formation due to mixed convection between two infinite vertical parallel plates with a transverse magnetic field. The dimensionless governing equations are reduced and solved to determine entropy generation and MHD flow effects. We analyzed the effects of velocity slip and temperature jump in the presence of a magnetic field, thermal radiation, and suction or injection on velocity field, volumetric flow rate, temperature distribution, skin friction coefficients, and entropy formation. The results show that changing magnetic, suction, or injection parameters changes fluid velocity at the solid-fluid interface.

Keywords— Entropy generation; Hydromagnetic flow; Exothermic fluid; Micro-channel.

I. INTRODUCTION

Natural convection processes are common in heat exchangers, petroleum reservoirs, combustion modelling, nuclear energy, fire engineering, etc., hence many researchers have concentrated on them. Electronics and supercomputers, micro-channel heat sinks, microdevices, electronic cooling, and other fields are interested in flow and natural convection in microchannels.

Thermal energy, cooling of modern electronic systems, geothermal energy systems, and solar power collectors have sparked interest in entropy generation minimization research. Analyzing entropy generation can determine if a thermal process is irreversible. Heat and mass transfer, friction, or chemical reaction can produce microfluidic flow irreversibility. Zahmatkesh et al. [1] recently explored the impact of entropy development on nanofluid flow approaching standstill. Ebrahimi et al. [2] study entropy creation and heat exchange with longitudinal vortex generation. Ibanez et al. [3] studied how magnetic field and entropy affected nanofluid flow in a microchannel. Fersadou et al. [4] examine mixed convection and entropy production in MHD nanofluid flow. Shi and Dong [5] discussed microchannel entropy and heat transmission. Nasiri et al. [6] studied how magnetic field impacts microchannel entropy. Jian [7] explored MHD flow in a microchannel with electroosmotic effects.

Adding a heat source reduces entropy in thermal conduction. et al. [8]. Ibanez et al. [9] studied how to reduce entropy in a solid slab using steady-state heating. By modifying the Biot number in one surface, they found an ideal Biot number for the second surface that minimises global entropy. Bertolo and Cafaro [10] studied lowest entropy production and heat and fluid movement. They found that a system's steady-state minimal entropy production cannot be negative. Basio [11] studied one-dimensional heat conduction using temperature-dependent thermal conductivity. Kareem et al. [12] studied the flow of a reactive internal irreversible MHD fluid with variable viscosity in a fixed exothermal wall. Entropy generation can be decreased at low viscosity and dissipation rate.

Heat and mass transfer via suction/injection have many engineering applications. Aerodynamics and space sciences benefited from boundary layer suction and injection. Shojaefard et al. [13] used suction/injection to modulate subsonic fluid flow. Flow control could reduce fuel consumption by 30%, pollutant emissions by 50%, and commercial aircraft operating expenses by 8%. [14] Suction or injection can drastically modify the flow field, which impacts plate heat transfer. Ishak et al. Griffith and Meredith [16] explored the flow of a viscous, incompressible fluid over infinite porous plates. Devi and Kandasamy [17] studied chemical reaction, heat transport, and mass transfer on non-linear MHD laminar boundary-layer flow over a wedge with suction or injection. Kandasamy et al. [18] studied the effects of chemical reaction, heat, and mass movement along a wedge with suction or injection. Kandasamy et al. [19] studied chemical reaction, heat, and mass transfer on boundary layer flow across a porous wedge with suction or injection.

Slip flow regime is significant in today's advanced technology and production. Near a solid surface, fluid doesn't adopt its speed. Surface tangential velocity is finite. Floor slides. Flow slip has serious consequences. Makinde and Osalusi [20] discussed slip's effect on hydromagnetic steady flow in a porous channel. Khalid and Vafai [21] developed closed form solutions for Newtonian fluid velocity fields at solid barriers. Watanabe et al [22] studied Navier slip in Newtonian fluids at solid barriers. Chen and Tian [23] explored entropy formation in thermal micro-Couette slip flows.

This article analyses the combined effects of Newtonian heating and Navier slip on steady exothermic fluid flow in a vertical channel. The governing equations have a closed-form solution. The impacts of physical parameters on temperature, entropy production, fluid velocity, and Bajan number are visually represented and analysed. Parallel plate shear stress and heat transfer rate are also estimated and modelled.

II. MATHEMATICAL ANALYSIS

Consider a steady state Magnetohydrodynamic free convection of an exothermic fluid with suction/injection, heat transfer, and Navier slip condition in a vertical channel formed by two infinite plates separated by a distance H^* (Figure 1). It is presumed that the channel walls are taken vertically parallel to $x -$ axis, parallel to gravitational force. Due to heating, it is also assumed that on one plate ($y^* = H^*$) fluid is injected into the channel with certain constant velocity S^* and that is sucked off from the other plate ($y^* = 0$) at the same rate. under the usual Boussinesq approximation, the non-dimensional governing equations are given as:

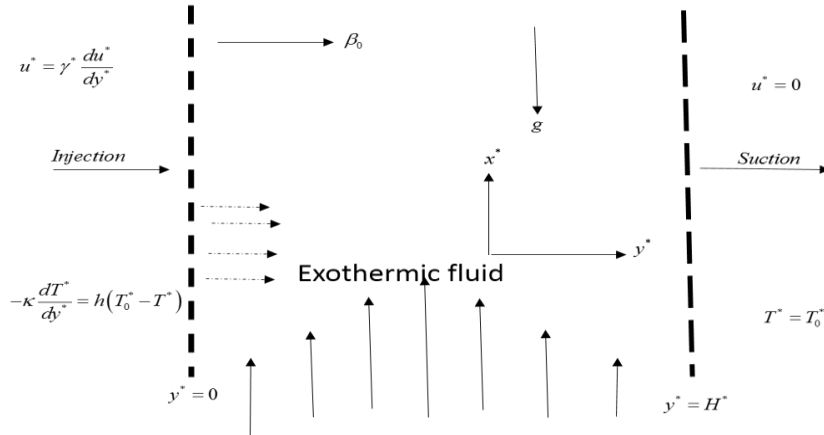


Figure 1: Geometry of the Problem

$$-S^* \frac{du^*}{dy^*} = \nu \frac{d^2u^*}{dy^{*2}} + g\beta_T(T^* - T_0^*) - \frac{\sigma\beta_0^2 u^*}{\rho} - \frac{\nu u^*}{\kappa^*} \tag{1}$$

$$-S^* \frac{dT^*}{dy^*} = \frac{\kappa}{\rho C_p} \frac{d^2T^*}{dy^{*2}} + \frac{Q_0 C_0^* A}{\rho C_p} e^{\left(\frac{-E}{RT^*}\right)} \tag{2}$$

The corresponding boundary conditions representing the slip conditions are:

$$\left. \begin{aligned} u^* = \gamma^* \frac{du^*}{dy^*}, -\kappa \frac{dT^*}{dy^*} = h(T_0^* - T^*), \text{ at } y^* = 0 \\ u^* = 0, T^* = T_0^*, \text{ at } y^* = H^* \end{aligned} \right\} \tag{3}$$

In other to non-dimensionalise eq. (1-3), we introduced the following non-dimensional variables:

$$\left. \begin{aligned} S = \frac{S^* H}{\nu}, Da = \frac{\kappa^2}{\nu H^2}, Pr = \frac{\nu \rho C_p}{\kappa}, \beta = \frac{H^*}{H}, Ha^2 = \frac{\sigma \beta_0^2 H^2}{\nu R \rho}, y = \frac{y^*}{H}, \\ \theta = \frac{E(T^* - T_0^*)}{RT_0^2}, \varepsilon = \frac{RT_0}{E}, \alpha = \frac{Q_0 C_0^* A E}{RT_0^2} e^{\frac{-E}{RT_0}}, Br = \frac{hH}{\kappa}, \gamma = \frac{\gamma^*}{H}, \\ u = \frac{u^* E \nu}{g \beta_T H^2 T_0^2}, \theta_0 = \frac{E(T_a - T_0)}{RT_0^2} \end{aligned} \right\} \tag{4}$$

Using eq. (4) on eq. (1-3) we've:

$$-S \frac{du}{dy} = \frac{d^2u}{dy^2} + \theta - b_1 u \tag{5}$$

$$-S Pr \frac{d\theta}{dy} = \frac{d^2\theta}{dy^2} + \alpha e^{\frac{\theta}{1+\varepsilon\theta}} \tag{6}$$

$$\left. \begin{aligned} u = \gamma \frac{du}{dy}, \frac{d\theta}{dy} = Br(\theta - \theta_a) \text{ at } y = 0 \\ u = 0, \theta = 0 \text{ at } y = \beta \end{aligned} \right\} \tag{7}$$

Where $\gamma, Br, Pr, \alpha, \theta$ and ε are Navier slip parameter, Biot number, Prandtl number, Frank-Kamenetskii parameter, ambient temperature and activation energy parameter.

III. SOLUTION OF THE PROBLEM

The steady state governing equations and their boundary condition corresponding to Eq. (5-7) can be re-written as:

$$\frac{d^2u}{dy^2} + S \frac{du}{dy} - b_1u = -\theta \tag{8}$$

$$\frac{d^2\theta}{dy^2} + S Pr \frac{d\theta}{dy} = -\alpha e^{\frac{\theta}{1+\varepsilon\theta}} \tag{9}$$

$$\left. \begin{aligned} u - \gamma \frac{du}{dy} = 0, \frac{d\theta}{dy} - Br(\theta - \theta_a) = 0 & \text{ at } y = 0 \\ u = 0, \theta = 0 & \text{ at } y = \beta \end{aligned} \right\} \tag{10}$$

To determine the approximate solutions of Eq. (8) and (9) subject to Eq. (10), we assume the power series expansion in the Frank-Kamenetskii parameter (α) of the form:

$$\left. \begin{aligned} u &= u_0 + \alpha u_1 + \dots \\ \theta &= \theta_0 + \alpha \theta_1 + \dots \end{aligned} \right\} \tag{11}$$

Substituting Eq. (11) into Eq. (8) and (9) subject to Eq. (10), neglecting higher orders of α and equating the coefficient of like powers of α , the resulting solutions of Eq. (8-9) are severally as follows:

$$u = E_1 e^{l_1 y} + E_2 e^{l_2 y} + E_3 + E_4 e^{-S Pr y} + E_5 y e^{-S Pr y} + E_6 e^{-2S Pr y} + E_7 e^{-3S Pr y} \tag{12}$$

$$\theta = n_1 + n_2 e^{-S Pr y} + n_3 y e^{-S Pr y} + n_4 e^{-2S Pr y} + n_5 e^{-3S Pr y} \tag{13}$$

Differentiating Eq. (12) and (13) with respect to y , we obtained respectively

$$u' = E_8 e^{l_1 y} + E_9 e^{l_2 y} - E_{10} e^{-S Pr y} - E_{11} y e^{-S Pr y} - E_{12} e^{-2S Pr y} - E_{13} e^{-3S Pr y} \tag{14}$$

$$\theta' = n_6 e^{-S Pr y} - n_7 y e^{-S Pr y} - n_8 e^{-2S Pr y} - n_9 e^{-3S Pr y} \tag{15}$$

The physical quantities of engineering interest such as Nusselt number, Skin friction, Entropy generation, volumetric flow rate and Bejan number are computed.

From Eq. (15), the rates of heat transfer at the beginning and end of the plate are respectively:

$$Nu_0 = n_6 - n_8 - n_9 \tag{16}$$

$$Nu_\beta = n_{10} e^{-S\beta Pr} - n_{11} e^{-2S\beta Pr} \tag{17}$$

Also, from Eq. (14), the Skin friction on the boundaries are as follows:

$$\tau_0 = E_8 + E_9 - E_{10} - E_{12} - E_{13} \tag{18}$$

$$\tau_\beta = E_8 e^{\beta l_1} + E_9 e^{\beta l_2} - E_{10} e^{-\beta S Pr} - E_{11} \beta e^{-\beta S Pr} - E_{12} e^{-2\beta S Pr} - E_{13} e^{-3\beta S Pr} \tag{19}$$

The non-dimensional volumetric flow rate is given by:

$$\text{Volumetric flow rate } (Q) = \int_0^\beta u dy$$

Using Eq. (12), we obtained

$$Q = \frac{n_{12} E_1}{E_1} + \frac{n_{13} E_2}{E_2} + n_{14} + \frac{n_{15} E_4}{S Pr} + \frac{n_{15}}{S^2 Pr^2} - n_{16} + \frac{n_{17} E_6}{2S Pr} + \frac{n_{18} E_7}{3S Pr} \tag{20}$$

By using Eq. (12), (14) and (15) the dimensionless form of Entropy number N_s can be written as:

$$N_s = (\theta')^2 + \frac{Br}{Pr} (u')^2 + \frac{Br}{Pr} M^2 u^2 \tag{21}$$

Also, using Eq. (15) the Bejan number is given by:

$$Be = \frac{(\theta')^2}{N_s} \tag{22}$$

IV. RESULTS AND DISCUSSION

Figures 2-12 show the effects of velocity, temperature, skin friction coefficient, entropy production, Nusselt number, Bejan number, and volumetric flow rate on the flow. The following values are fixed for the regulating parameters,

$\gamma = 0.1, \varepsilon = 0.01, \alpha = 0.01, Br = 0.01, \theta_a = 1, Da = 1.0, M = 0.5$, also, the values of S lies between $-2 \leq S \leq 2$, the value of Pr is taken as 0.71.

Figure 2 shows the effect of Magnetic parameter (M) on the velocity profile. The velocity of the fluid decreases as magnetic parameter (M) increases and vice versa. This is expected since the introduction of magnetic field to an electrically conducting fluid gives rise to Lorentz force. Fluid velocity drops. Figure 3 shows the impact of suction/injection (S) on fluid flow. As suction parameter increases, fluid velocity decreases. Injection parameter increases fluid velocity.

Figure 4 shows that increasing the suction/injection parameter (S) decreases the fluid's temperature profile. This is because cold fluid particles are injected into the channel through the cold wall while hot fluid particles are removed, which decreases the channel temperature and the fluid's temperature. Increasing the slip parameter (γ) increases the fluid velocity at the lower plate surface (Figure 5). Figure 6 shows Darcy parameter's (Da) impact on flow rate. Increasing Darcy parameter's (Da) decreases the volume flow rate. Figure 7 shows how suction/injection parameter (S) affects volume flow rate. For higher values of values of suction/injection parameter (S), volume flow rate falls dramatically.

Figure 8 shows the effects of suction/injection parameter (S). Entropy generation is higher near the cold plate than the hot plate, indicating that the temperature gradient is lower near the hot plate. Suction/injection parameters (S), reduce entropy. Figure 9 shows the impact of Biot number (Br) on entropy generation profile. The maximum entropy is generated at the cold plate compared to the hot plate.

Figure 10 depicts the impact of Brickman's number ($\frac{Br}{\Pi}$) on entropy generation profile. As Brickman's number increases, entropy is generated, but the increment is more noticeable at the cold plate. Figure 11 shows the influence of suction/injection parameter (S) on Nusselt number (Nu). The rate of heat transmission at the hot plate increases as the suction/injection parameter (S) increases. For higher values of the suction/injection parameter (S), the rate of heat transfer is uniform.

Figure 12 shows the influence of suction/injection parameter (S) on skin friction (Sk) at the first channel wall. An increase in suction/injection parameter (S) reduces flow skin friction (Sk). Figure 13 shows the effect of magnetic parameter (M) on Bejan number (Be), which grows at the first wall, reduces in the middle, and increases towards the second.

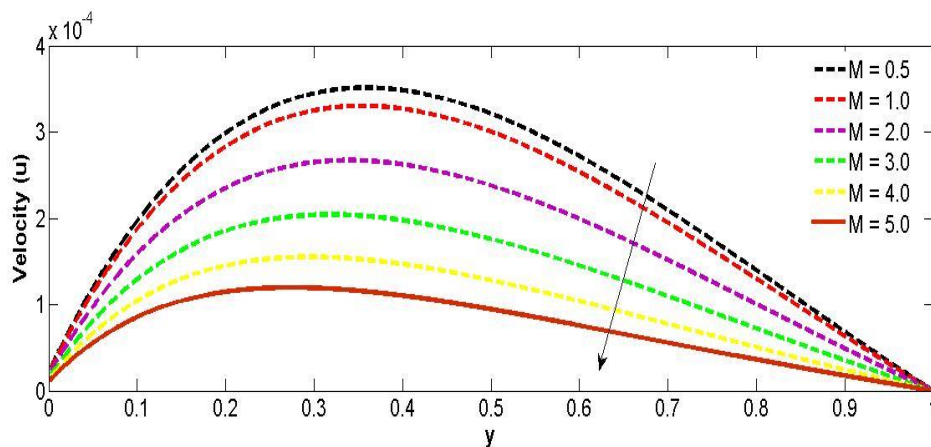


Figure 2: Effect of Magnetic Parameter (M) On Velocity Profile

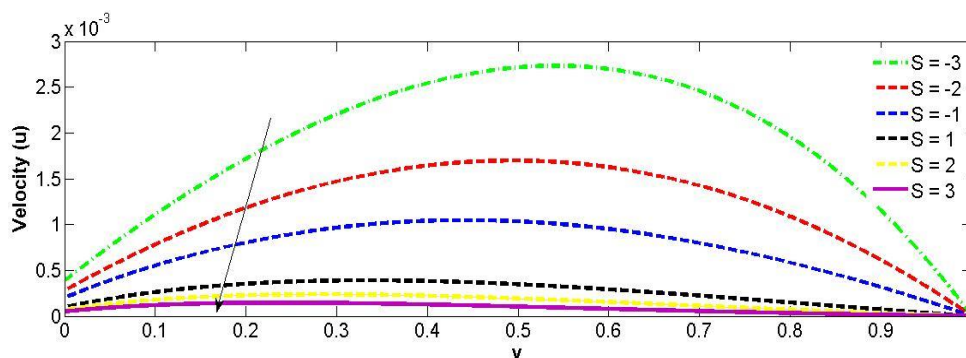


Figure 3: Effect of Suction/ Injection Parameter (S) On Velocity Profile

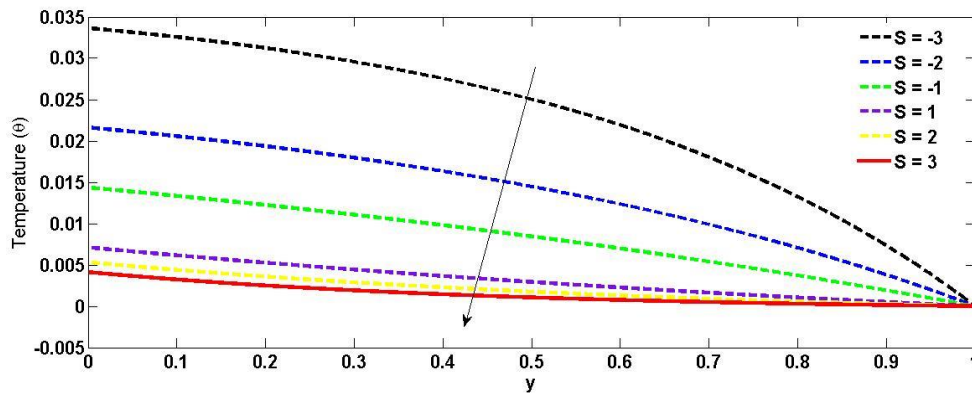


Figure 4: Effect of Suction/ Injection Parameter (S) On Temperature Profile

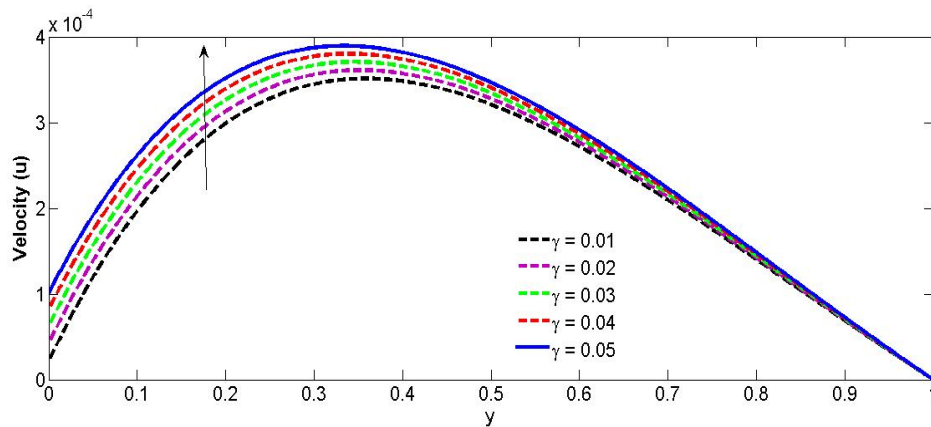


Figure 5: Effect of Slip Parameter (γ) on Velocity Profile

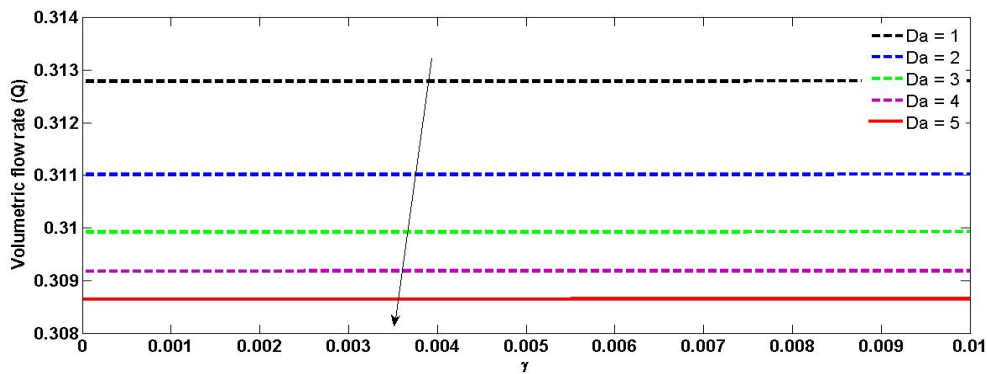


Figure 6: Effect of Darcy number (Da) on volumetric flow rate profile

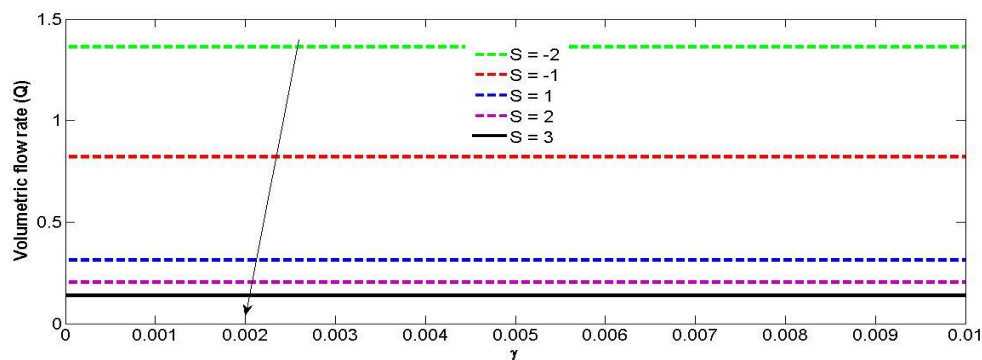


Figure 7: Effect of Suction/ Injection parameter (S) on volumetric flow rate profile

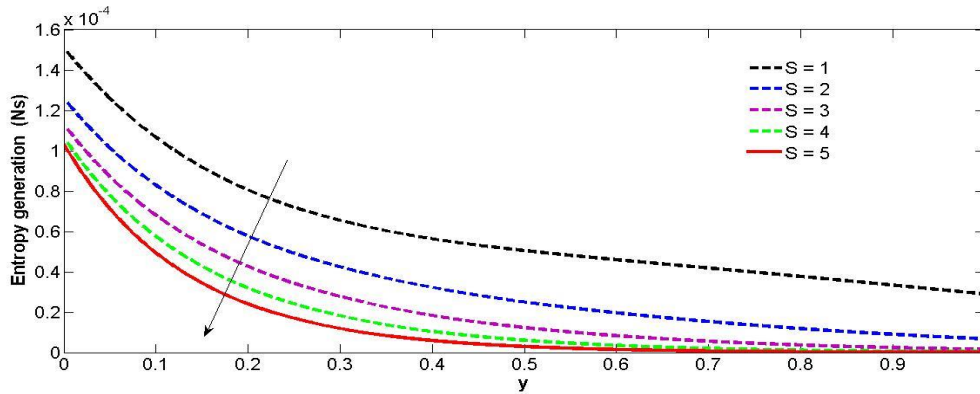


Figure 8: Effect of Suction/ Injection (S) on Entropy generation

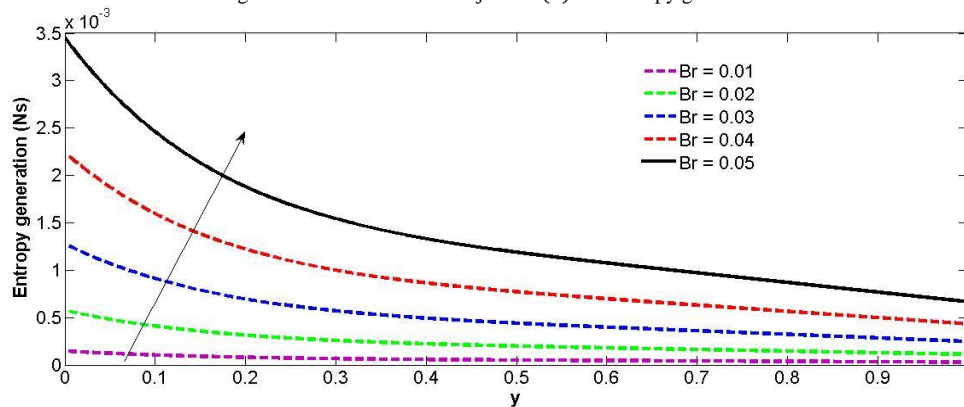


Figure 9: Effect of Biot number (Br) on Entropy generation profile

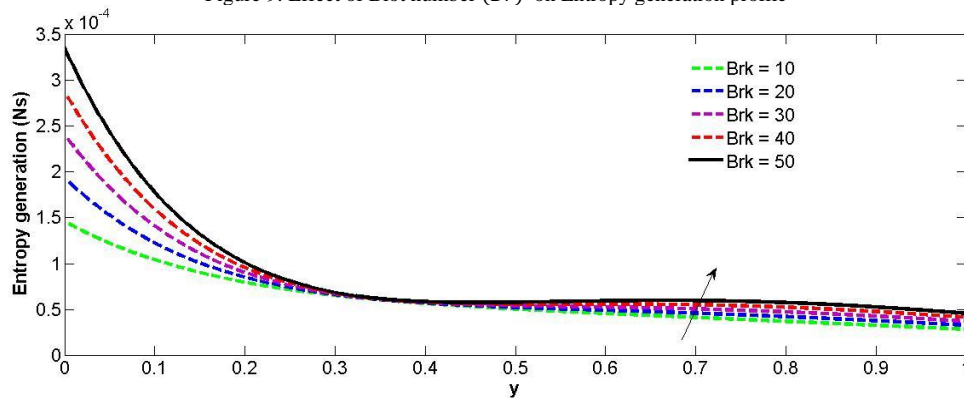


Figure 10: Effect of Brickman number (Brk) on Entropy generation profile

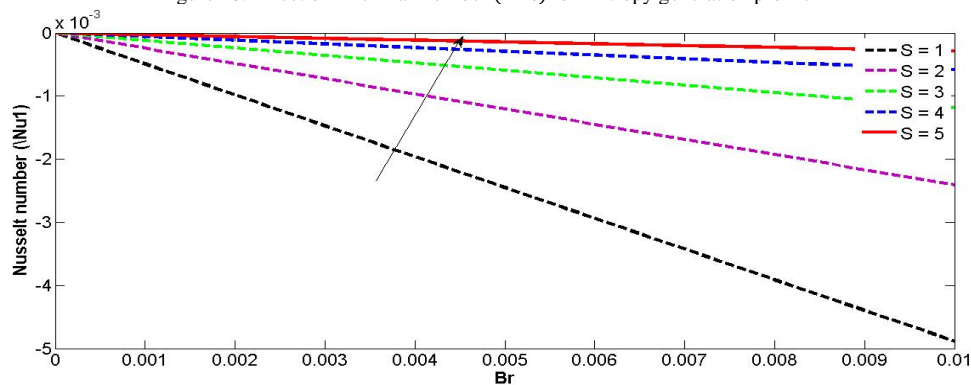


Figure 11: Effect of Suction/ Injection parameter (S) on Nusselt number profile

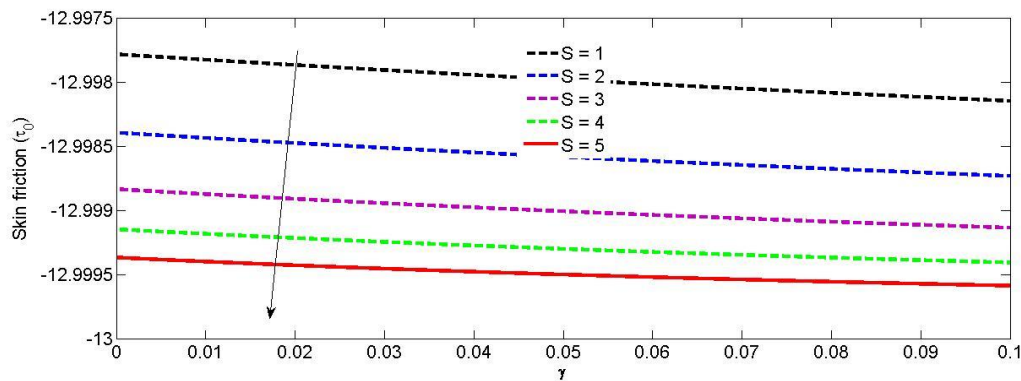


Figure 12: Effect of Suction/ Injection (S) on Skin friction profile

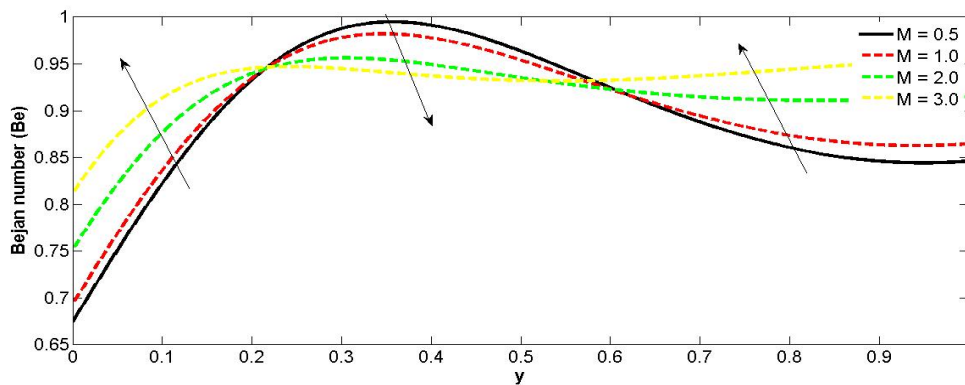


Figure 13: Effect of Magnetic parameter (M) on Bejan number profile

V. CONCLUSIONS

Entropy generation in a vertical infinite parallel channel trenched with permeable medium in the existence of aligned magnetic field, partial slip and suction/injection have been studied and analyzed. The effects of the pertinent parameters on the temperature and velocity are investigated and analysed with the help of their graphical representations. From the results the following conclusions could be drawn:

- (i) The fluid velocity increases with an increase in the Navier slip parameter (γ), magnetic parameter (M) and suction/injection (S).
- (ii) The volumetric flow rate decreases with varying values of Darcy parameter (Da) and suction/injection (S).
- (iii) The entropy generation enhanced with an increase in the Biot number (Br) and Brickman number (Brk) while it declined with suction/injection (S).
- (iv) The skin friction is decayed while Nusselt number growth with an increase in the suction/injection parameter (S).

REFERENCES

- [1] R. Zahmtkesh, H. Mohammadiun, M. Mohammadiun, M.H.D. Bonab, Investigation of entropy generation in nanofluid's axisymmetric stagnation flow over a cylinder with constant wall temperature and uniform surface suction-blowing, *Alex. Eng. J.* 58 (2019) 1483–1498.
- [2] A. Ebrahimi, F. Rikhtegar, A. Sabaghan, E. Roohi, Heat transfer and entropy generation in a microchannel with longitudinal vortex generators using nanofluids, *Energy* 101 (2016) 190–201.
- [3] G. Ibanez, A. Lopez, J. Pantoja, J. Moreira, Entropy generation analysis of a nanofluid flow in MHD porous microchannel with hydrodynamic slip and thermal radiation, *Int. J. Heat Mass Transf.* 100 (2016) 89–97.
- [4] I. Fersadou, H. Kahalerras, M. El. Ganaoui, MHD mixed convection and entropy generation of a nanofluid in a vertical porous channel, *Comp. Fluids* 121 (2015) 164–179.
- [5] Z. Shi, T. Dong, Entropy, generation and optimization of laminar convective heat transfer and fluid flow in a microchannel with staggered arrays of pin fin structure with tip clearance, *Energy Conser. Mang.* 94 (2015) 493–504.
- [6] M. Nasiri, M.M. Rashidi, G. Lorenzini, Effects of magnetic field on entropy generation in a microchannel heat sink with offset fan shaped, *Entropy* 17 (2015).
- [7] Y. Jian, Transient MHD heat transfer and entropy generation in a micro parallel channel combined with pressure and electroosmotic effects, *Int. J. Heat Mass Transf.* 89 (2015) 193–205.
- [8] Kolande, Z., Donizak, J. and Hubert, J. (2004). On the minimum entropy production in steady state heat conduction processes. *Entropy*, 29:2441-2460.
- [9] Ibanez, G., Cuevas, S. and Lopez de Hara, M. (2003), minimization of entropy generation by asymmetric convective cooling. *Int. J. Heat Mass Transf.* 42: 1321-1328.
- [10] Bertolo, V. and Cafaro, E. (2008). A critical analysis of the minimum entropy production theory and its application to heat and fluid flow. *Int. J. Heat Mass Transf.* 51: 1907-1912.
- [11] Bisio, G. (1990). Entropy production rate in the one-dimensional heat conduction for systems whose thermal conductivity or its derivative are piecewise continuous with respect to temperature. *Worme und stoffubtragung*, 25: 117-127.

[12] Khaleed, A.R.A. (2008), conduction and entropy transfer in a semi-infinite medium and wall with a combined periodic heat flux and convective boundary condition. *Intl. J. Thermal Sci.* 47:76-83.

[13] Kareem, R.A., Salawu, S.O. and Yan, Y. (2020). Analysis of transient Rivlin-Erickson fluid and irreversibility of exothermic reactive hydromagnetic variable viscosity. *J. Appl. Comput. Mech.* 6(1), 26-36

[14] Shajaeferd, M. H., Noorpoor, A. R., Avanesians, A. and Ghaffapour, M. (2005), Numerical investigation of flow control by suction and injection on a subsonic airfoil, *The American Journal of Applied Sciences*, Vol. 20, pp. 1474-1480.

[15] Braslow, A. I. (1999), a history of suction type Laminar flow control with emphasis on flight research, *American Institute of Aeronautics and Astronautics*, Washington, Wash, USA.

[16] Ishak, A., Nazar, R. and Pop, I. (2008). Mixed convection boundary layer flow over a permeable vertical surface with prescribed wall heat flux, *Zeitschrift für angewandte Mathematik und Physik*, Vol.59, no.1, pp. 100-123.

[17] Griffit, A. A. and Meridith, F. W. (1936), the possible improvement in Aircraft performance due to use of boundary layer suction. *Aeronautical Research Council*, London, UK.

[18] Devi, S. P. A. and Kandasamy, R. (2022) studied effects of chemical reaction, heat and Mass transfer on non-linear MHD Laminar boundary- layer flow over a wedge with suction or injection, *International Communications in Heat and Mass Transfer*, 29(5), 707-716.

[19] Kandasamy, R., Periasamy, K. and Prabhu, K. K. S. (2005), effects of chemical reaction, heat and mass transfer along a wedge with heat source and concentration in the presence of suction or injection, *International Journal of Heat and Mass transfer*, 48(7), 1388-1394.

[20] Kandasamy, R., Raj, A. W. B. and Khamis, A. B. (2006), effects of chemical reaction, heat and mass transfer on boundary layer flow over a porous wedge with heat radiation in the presence of suction or injection, *Theoretical and Applied Mechanics*, 33(2), 123-148.

[21] Makinde, O.D. and Osalusi, E. (2006), MHD steady flow in a channel with slip at the permeable boundaries. *Rom J Phys*, 51, 319-328.

[22] Khalid, A. R. A. and Vafai, K. (2004), the effect of the slip condition on Stokes and Couette flow due to an oscillatory wall: exact solution, *Intl J NonLin Mech*, 39, 795-809.

[23] Watanebe, K. and Yanuar, M.H. (1998), slip of Newtonian fluid at solid boundaries, *J Jpn Soc Mech Eng*, 341-525.

[24] Chen, A. and Tian, Z. (2010), entropy generation analysis of thermal micro- Couette flow in slip regime, *Int J Therm Sci*, 49, 2211-2221.

APPENDIX

$$E_1 = C_1 + \alpha m_1; E_2 = C_2 + \alpha m_2; E_3 = C_3 + \alpha N_1; E_4 = C_4 + \alpha N_2; E_5 = N_3 \alpha; E_6 = N_4 \alpha;$$

$$E_7 = N_5 \alpha; E_8 = l_1 E_1; E_9 = l_2 E_2; E_{10} = E_4 S Pr - E_5; E_{11} = E_5 S Pr; E_{12} = 2E_6 S Pr; E_{13} = 3E_7 S Pr$$

$$n_1 = A_1 + \alpha B_0; n_2 = A_2 + \alpha B_2; n_3 = \alpha D_2; n_4 = \alpha D_3; n_5 = \alpha D_4; n_6 = n_3 - n_2 S Pr; n_7 = n_3 S Pr;$$

$$n_8 = 2n_4 S Pr; n_9 = 3n_5 S Pr; n_{10} = n_6 - n_7 \beta; n_{11} = n_8 + n_9 e^{-S Pr}; n_{12} = e^{\beta l_1} - 1; n_{13} = e^{\beta l_2} - 1$$

$$n_{14} = E_3 \beta; n_{15} = 1 - e^{-\beta S Pr}; n_{16} = \frac{\beta e^{-\beta S Pr}}{S Pr}; n_{17} = 1 - e^{-2\beta S Pr}; n_{18} = 1 - e^{-3\beta S Pr}$$

Greek Letters

β_T	Coefficient of thermal expansion
κ	Thermal conductivity
g	Acceleration due to gravity
ρ	Density of the fluid
ν	Kinematic viscosity
σ	Electrical conductivity
C_p	Specific heat capacity
A	Rate of reaction

List of Symbols

γ	Navier Slip parameter
Q_0	Heat of reaction
S^*	Constant suction/injection velocity
u	Dimensionless velocity
M	Magnetic parameter
E	Activation energy
α	Frank-Kamenetskii parameter
R	Universal constant
θ	Dimensionless temperature of the fluid
T'	Temperature of the fluid
S	Suction/injection parameter
u	Dimensionless Velocity of the fluid
Da	Darcy number
u^*	Dimensional velocity of the fluid
Be	Bejan number
$\frac{Br}{\Pi}$	Brinkman number, = $Er \times Pr$
Pr	Prandtl number
Q	Volumetric flow rate
Br	Biot number
T_0	Constant ambient temperature